Molecular and histopathologic characteristics of radioiodine-refractory papillary thyroid cancer

Ju Yeon Pyo

Department of Medicine

The Graduate School, Yonsei University

Molecular and histopathologic characteristics of radioiodine-refractory papillary thyroid cancer

Directed by Professor SoonWon Hong

The Doctoral Dissertation
submitted to the Department of Medicine,
the Graduate School of Yonsei University
in partial fulfillment of the requirements for the degree
of Doctor of Philosophy

Ju Yeon Pyo

December 2015

This certifies that the Doctoral Dissertation of Ju Yeon Pyo is approved.

Thesis Supervisor : SoonWon Hong

Thesis Committee Member#1 : Hang-Seok Chang

Thesis Committee Member#2 : Jae Yong Cho

Thesis Committee Member#3: Chan-Kwon Jung

Thesis Committee Member#4: Beom Jin Lim

The Graduate School
Yonsei University

December 2015

ACKNOWLEDGEMENTS

I am extremely grateful to Professor SoonWon Hong who has patiently guided me while preparing my thesis and supported me at all time as my mentor in life. I gratefully acknowledge Professor Hang-Seok Chang, Professor Jae Yong Cho, Professor Chan-Kwon Jung, and Professor Beom Jin Lim for their knowledgeable and practical advice.

I would like to express my gratitude to the faculty and colleagues of the Department of Pathology, Yonsei University College of Medicine who brought me here and helped me. I also express my gratitude to the faculty and staffs of the Department of Pathology, Hanyang University Guri Hospital for their encouragement and support.

I am particularly expressing my gratitude to Hyeongjae Jeong, Jae Yun Lim, Professor Eunah Shin, for their wholehearted instruction and help with my experiments. I also thank Yeon ji Park and Su Mi Park who kindly granted my urgent requests.

I would like to express my deepest gratitude to my mother and aunt Ji-hyun for providing their wholehearted devotion with endless support and love, and Reverend Ho-tak Jeong, and my parents-in-law for providing endless support and pray for me. I also thank my loving husband, Yoon Seop So who is always supportive of me, my lovely son, Jae Yoon, my considerate sisters, and reliable brother. Finally, I am thankful to our Heavenly Father who always looks all around carefully.

Ju Yeon Pyo

<TABLE OF CONTENTS>

LIST OF FIGURES

LIST OF TABLES

ABSTRACT

Molecular and histopathologic characteristics of radioiodine-refractory papillary thyroid cancer

Ju Yeon Pyo

Department of Medicine
The Graduate School, Yonsei University

(Directed by Professor SoonWon Hong)

Radioiodine (RI) ablation after surgery with suppression of thyroid-stimulating hormone is an effective therapy for papillary thyroid cancer (PTC) and leads to an excellent prognosis. However, RI-refractory tumors are aggressive and have poor outcomes. Recently, studies of genetic abnormalities associated with signaling pathways related to PTC have shown that activation and mutation of telomerase reverse transcriptase (*TERT*) activity is associated with a poor outcome in PTC. We analyzed the proportion of mutations in *BRAF* V600E and the *TERT* promoter, and compared the clinicopathological differences between RI-refractory and RI-responsive PTCs. Among 82 patients of RI-refractory PTC, we identified 26 cases for which formalin-fixed, paraffin-embedded tissue from the initial thyroidectomy were available. In the matched RI-responsive group without distant metastasis in the 5

years after surgery, 89 cases of PTC were collected.

In the histopathological comparison of the two groups, RI-refractory PTCs showed a significant increase in small tumor clusters without fibrovascular cores (≥ 20% cut-off, especially in tumor centers), hobnail features (≥ 5% cut-off, especially in tumor centers), and in the height/width ratio of tumor cells (maximum ≥ 3). RI-refractory PTC showed significantly increased frequency of tumor necrosis, mitosis, lymph node metastasis, extrarthyroidal tumor extension, and involvement of resection margin. Interestingly, the nuclei of RI-refractory PTCs had an increased tendency to be located between the base and the middle area of tumor cells. *TERT* promoter mutations were found in 14/26 cases of RI-refractory PTC (53.8%, 13 *TERT* C228T, 1 *TERT* C250T) whereas only 1/82 cases of RI-responsive PTC showed *TERT* promoter mutations (1.2%, *TERT* C228T). The *BRAF* V600E mutation was identified in more than 80% of cases in both groups. Coexistence of *TERT* promoter and *BRAF* mutations was found in 13/108 (12%) of all PTC cases. *TERT* promoter mutations were significantly associated with clinicopathologic features mentioned above. Immunohistochemically, expression of NIS and TSHR was decreased in many cases of RI-refractory PTC. The expression of VEGF, VEGFR2, and NF-κB, known to be oncogenic

proteins, was somewhat lower in RI-refractory PTC than in RI-responsive PTC. Total loss of expression of PTEN was occasionally present in both groups. β-catenin, which is involved in the WNT-β-catenin pathway, showed cytoplasmic positivity in all cases. Comparison of immunohistochemical results for *TERT* and *BRAF* mutations in all PTCs showed no correlation with either mutation, except for TSHR (*TERT* mutation). Four significant predictors of RI-refractoriness were identified: *TERT* mutation, height/width of tumor cells > 3, increased small clusters (≥ 20%), and necrosis.

Our results suggest that RI-refractory PTCs may be strongly associated with *TERT* mutations and aggressive histopathologic features (small clusters and hobnail components), especially in tumor centers.

Key words: Papillary thyroid cancer, radioiodine-refractory, *TERT* promoter mutations, micropapillary, hobnail, immunohistochemistry

Molecular pathogenesis and histopathologic characteristics of radioiodine-refractory papillary thyroid cancer

Ju Yeon Pyo

Department of Medicine
The Graduate School, Yonsei University

(Directed by Professor SoonWon Hong)

I. INTRODUCTION

Papillary thyroid carcinoma (PTC) is the most common type of malignant thyroid neoplasm and its incidence has increased remarkably in recent years.[1,2] Conventionally, the standard treatment for thyroid cancer is total or near-total thyroidectomy and adjuvant radioiodine (RI) ablation with suppression of thyroid stimulating hormone (TSH).[3] Physiologically, thyroid follicular cells trap iodine using a sodium–iodide symporter (natrium iodide symporter, NIS), an energy-dependent transport system regulated by TSH[4]. Iodine is organified by thyroid peroxidase (TPO) at the apical surface of thyroid cells and then conjugated to thyroglobulin (Tg). Iodine is also trapped and organified by differentiated thyroid cancer (DTC) cells, as in thyrocytes.[5] Iodine-131 (^{131}I) is a β- and γ-emitting radionuclide and an effective therapeutic and imaging agent for DTCs. Dedifferentiated, poorly differentiated, and anaplastic thyroid tumor cell clones have lost the ability to trap iodine. Thus, RI is not effective for

detection or therapy of these tumors. Non-RI avid tumors have aggressive behavior and a poor prognosis.[6] The classic treatment approach is highly effective for DTC, as DTC usually has an excellent prognosis with a 10-year disease-related survival of 85%.[7] However, some patients with DTC develop an aggressive disease with distant metastases and loss of ^{131}I avidity. Patients with RI-resistant DTC are usually not responsive to conventional chemotherapy and have a long-term overall survival of 10%.[8] In addition, age, gender, tumor histological type, clinicopathological features, disease stage, presence of distant metastasis, and molecular genetic alterations may be responsible for the aggressive course of the disease. Molecular profiling of thyroid cancers is important for determination of prognosis, causes of treatment resistance, and targeted therapy options especially in RI-refractory patients.[8]

Recently, our understanding of the molecular pathogenesis of thyroid cancers has significantly improved, facilitating development of more effective targeted therapies, in particular tyrosine-kinase inhibitors. This mainly results from identification of the molecular alterations involved in thyroid cancer, including genetic and epigenetic alterations and dysregulation of signaling pathways,[8] such as the RAS-RAF-MEK-MAPK-ERK pathway, the mitogen-activated protein kinase (MAPK) pathway, and the phosphatidyl-inositol3-kinase-Akt (PI3K-AKT) pathway,[11] in addition to RET/PTC and TRK rearrangements. These mutually exclusive mutations are found in more than 70% of papillary

thyroid carcinomas, including *BRAF* and *RAS* point mutations; *RET/PTC* and *PAX8/PPARγ* gene rearrangements; alteration of the MAPK, PI3K, p53, Wnt-β catenin, hypoxia inducible factor-1α (HIF1-α), and nuclear factor-κB (NF-κB) signaling pathways; and microRNA profiles and aberrant methylation.[10-14]

The *BRAF* V600E mutation is caused by a T1799A transversion at exon 15, resulting in the replacement of valine (V) with glutamic acid (E) at position 600 of the protein, which results in expression of the BRAF-V600E mutant protein and causes activation of serine/threonine kinases.[11,15] *BRAF* mutations are the most frequent genetic alteration in PTC and develop exclusively in PTC and PTC-derived anaplastic thyroid cancers. The mutations are known to be highly prevalent in PTC, at a frequency of 44–90%.[16] A previous comprehensive multicenter study demonstrated a strong association of *BRAF* V600E with poor clinicopathologic outcomes of PTC, including aggressive pathological features, increased recurrence, loss of RI avidity associated with alteration of function of NIS, and treatment failures.[11,17] All of the rearrangements and mutations increase BRAF activity and cause continuous induction of the MAPK signaling pathway.[9]

The PI3K/Akt signaling pathway plays major roles in several cellular events involved in growth, proliferation, and apoptosis.[6] Activation of this pathway leads to tumorigenesis.[18] The role of the PI3K/AKT pathway was first revealed by the finding that Cowden's syndrome is caused by mutations or deletions of

the tumor suppressor gene *PTEN*. Activated Akt induces a signaling cascade by phosphorylating downstream protein effectors. Decreased expression or inactivation of the tumor suppressor gene product PTEN and activation by *RAS* oncogenes have also been described to activate the PI3K/Akt signaling pathway and play a role in thyroid tumorigenesis.[19] Combinations of some of these PI3K/Akt genetic alterations, as well as combination of these alterations with *BRAF* mutation, were shown to be present in more aggressive thyroid tumors. Genetic alterations that activate both the MAPK and PI3K/Akt pathways were also shown to be present.[11]

The MAPK pathway plays a major role in regulating cellular events, such as proliferation and survival, and is also known to affect tumorigenesis. Genetic and epigenetic alteration of the RTK (receptor tyrosine kinase)-RAS-RAF-MEK-MAPK-ERK pathway is very common in PTC.[9] *RET/PTC* rearrangements and point mutations in *RAS* and *BRAF* have been shown to activate the MAPK pathway.[10] In addition, secondary molecular events, such as hypomethylation and genome-wide hypermethylation[20] and up-regulation of several oncogenic proteins, such as chemokines, NF-κB,[21] HIF1-α, vascular endothelial growth factor (VEGF), matrix metalloproteinases (MMPs), MET, vimentin, prokineticin 1 (PROK1; also known as EG VEGF), prohibitin, thrombospondin 1 (TSP1), urokinase plasminogen activator (uPA) and its receptor (uPAR), and transforming growth factorβ1 (TGFβ1), drive

cancer cell growth, proliferation, and survival, together with tumor angiogenesis, invasion, and metastasis.[9] NF-κB has recently been shown to play an important role in thyroid cancer, for its ability to control the proliferative and antiapoptotic signaling pathways of thyroid neoplastic cells. The oncogenic proteins RET/PTC, RAS, and BRAF can induce NF-κB activation in papillary, follicular, and medullary thyroid carcinomas. A number of NF-κB inhibitors have been demonstrated to induce antiproliferative effects and/or massive apoptosis, especially in combination with radio- or chemotherapy. [21,22] Thyroid tumors are associated with high vascularization and high levels of VEGF.[23] Thyroid cell cultures show reduced proliferation when the VEGF pathway is blocked, thus demonstrating that antiangiogenic drugs have a direct antitumor activity on thyroid tumor cells.[24]

The WNT-β-catenin pathway has a well-established role in the regulation of cell growth and proliferation. Up-regulated β-catenin is translocated into the nucleus where it triggers transcription of various tumor-promoting genes. Point mutations in exon 3 of *CTNNB1* have been found in 66% of ATCs and 25% of poorly differentiated carcinomas, although not in DTCs. Thus, the WNT–β-catenin pathway seems to have a particularly important role in thyroid tumor aggressiveness.[25] Interestingly, RET–PTC can activate the WNT–β-catenin pathway by activating the PI3K–AKT pathway and also by directly phosphorylating β-catenin in thyroid cancer cells.[9]

The main function of follicular thyroid cells is to use iodide to synthesize thyroid hormone. Iodide is transported into the cell through sodium–iodide symporters (NIS) located in the basal membrane. NIS is up-regulated by TSH-mediated activation of TSHR.[26] The iodide-handling machinery is often impaired, particularly in advanced thyroid cancers, making RI treatment ineffective.[9] Aberrant activation of the MAPK pathway plays an important role in the impairment of the iodide-handling machinery.[16] *BRAF* V600E mutation is associated with the loss of RI avidity and with RI treatment resistance in PTC. In addition, *BRAF* V600E mutation is highly prevalent (78–95%) in recurrent RI-refractory PTC[28] but not in primary PTC (45%).[27] Several studies have reported *BRAF* V600E mutation, accompanied by decreased or absent expression of thyroid iodide-handling genes such as *NIS*, *TSHR*, *TPO*, *TG,* and *SLC26A4,* in thyroid cancer.[28-30] NIS expression is significantly lower in the tall cell and diffuse sclerosing variants of PTC than in conventional PTC. Due to their low NIS expression, the tall cell and diffuse sclerosing variants of PTC require higher cumulative doses of radioactive iodine therapy to improve the prognosis.[31] Activation of the PI3K-AKT pathway has also been shown to down-regulate the iodide-handling machinery. Inhibition of the PI3K-AKT pathway induces NIS expression[32] and also induces the expression of *TSHR*, *TPO,* and *TG,* and is enhanced by treatment with histone deacetylase inhibitors, in human thyroid cancer cells. The involvement of both the MAPK and

PI3K-AKT pathways in the silencing of thyroid iodide-handling genes is consistent with the accumulation of genetic alterations in both pathways as thyroid tumors progress, during which loss of RI avidity increases.[9]

Most recently, activation of telomerase, especially mutation and increase of telomerase reverse transcriptase (*TERT*) activity, was reported in thyroid cancer and several human solid tumors.[33-39] Telomerase synthesizes tandem repeats of TTAGGG at the ends of chromosomes in vertebrates and prevents chromosome shortening and loss of genetic information. A C>T mutation in the *TERT* promoter region increases *TERT* transcriptional activity.[40] Mutations in the *TERT* promoter, such as –chr5:1 295 228C>T (termed *TERT* C228T) and chr5:1 295 250C>T (termed *TERT* C250T), transform DTC to undifferentiated anaplastic carcinoma.[41] The frequency of *TERT* promoter mutation varies depending on the histologic subtype or differentiation of thyroid cancer (7.5–25%),[39] and it causes more aggressive behavior with poorer outcome in PTCs and is more frequent in *BRAF*-mutated tumors.[33,34]

In this study, we focused on well-known genetic abnormalities associated with signaling pathways and the related histopathologic features known in PTCs. We performed comparative analysis of the molecular changes and histopathologic differences between RI-responsive and RI-refractory PTCs. We aimed to identify clinicopathological features associated with the prognosis and treatment of RI-refractory PTCs.

II. MATERIALS AND METHODS

1. Case selection and clinicopathologic review

Formalin-fixed, paraffin-embedded (FFPE) tissue samples were obtained from PTC specimens obtained from patients who underwent thyroidectomy with RI and further treatment at Gangnam Severance Hospital (Seoul, Korea) between July 2006 and October 2014. Patient information and clinicopathological parameters were reviewed for 15,000 cases of PTC and analyzed retrospectively using the electronically available clinical data. A patient was considered resistant to the RI ablation therapy when at least one tumor lesion was observed that did not show uptake of RI, or when the lesion radiologically progressed in the first 12 months post-radioiodine administration, or when the patient had persistent disease following the administration of an accumulated dose of radioactive iodine of >600 mCi.[42] For this study, 82 cases of PTC were determined to belong to the RI-refractory group, which developed recurrence or distant metastasis following the administration of an accumulated dose of radioactive iodine of >600 mCi. After case sampling of the RI-resistant group, 89 cases of PTC were selected as age- and gender-matched case-controls without distant metastasis during 5 years and were sampled as the RI-responsive group. Among the RI-refractory group, FFPE tissue from initial thyroidectomy samples was obtainable in 26 cases.

A histopathologic review was performed on primary surgically removed

thyroid tissue and as much additional tissue as possible was obtained from both groups. According to the criteria recommended by World Health Organizing Classification of Tumors,[43] PTC was classified and staged according to AJCC Cancer Staging Manual, 7th edition.[44]

2. Mutational analysis using molecular studies

Sections (10 μm) were cut from the FFPE tissue blocks. DNA was extracted from these sections using the QIAamp DNA FFPE Tissue Kit (Qiagen, Hilden, Germany) according to the manufacturer's instructions. The extracted DNA was used in molecular assays using PNA-mediated clamping PCR and pyrosequencing methods.

PNA-mediated clamping PCR was performed using the PNA Clamp BRAF Mutation Detection kit (Panagene, Daejeon, Korea).[45] The real-time PCR reaction for the PNA clamping PCR was performed using a CFX 96 Real-time PCR System (Bio-Rad, Pleasanton, CA). PCR cycling conditions consisted of a 5 min hold at 94°C, followed by 40 cycles of 94°C for 30 sec, 70°C for 20 sec, 63°C for 30 sec, and 72°C for 30 sec. The Δ Ct (ΔCt) value was calculated by subtracting the Ct value of a tested sample from the standard Ct value of the clamping control sample ([Standard Ct] − [Sample Ct] = ΔCt). A cut-off ΔCt value ≥ 2 was considered positive for the *BRAF* mutation (Figure 1).

Pyrosequencing was performed for further analysis of *TERT* promoter

mutations. Pyrosequencing of *TERT* promoter mutations was performed with a sequencing primer (5′-ACCCCGCCCCGTCCC GACCCC-3′) on a Pyromark Q24 (Qiagen) after PCR amplification with the following primer pair (forward 5′-GTCCTGCCCCTTCACCTT-3′ and reverse 5′-biotin-CAGCGCTGCCTG AAACTC-3′) on a PCR C1000 Thermal cycler (Bio-Rad). The pyrogram output was analyzed using the PyroMark Q24 software (Qiagen) to determine the percentage of mutant versus wild-type DNA, according to relative peak height (Figure 2).

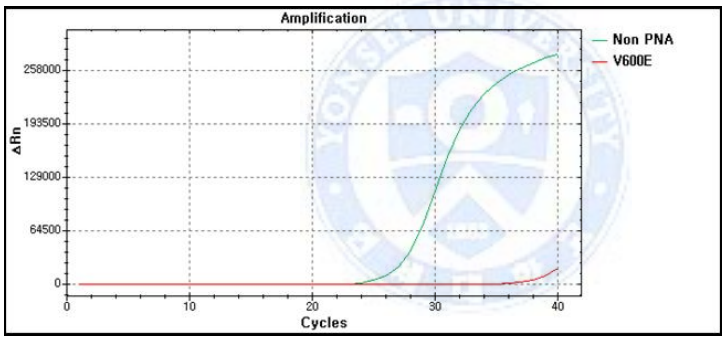

***BRAF* Negative control**

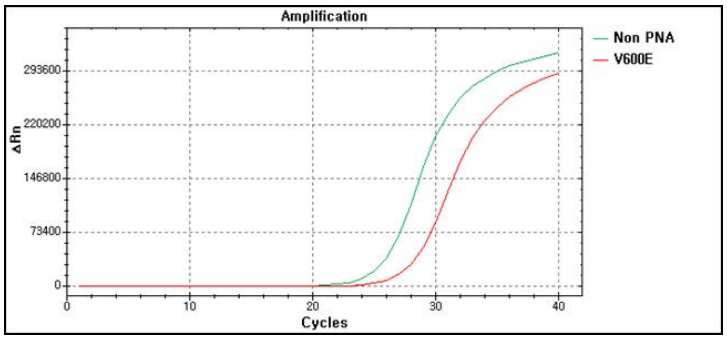

***BRAF* Test**

Figure 1. Results of PNA-mediated clamping PCR for *BRAF* mutatio

***TERT* – Negative control**

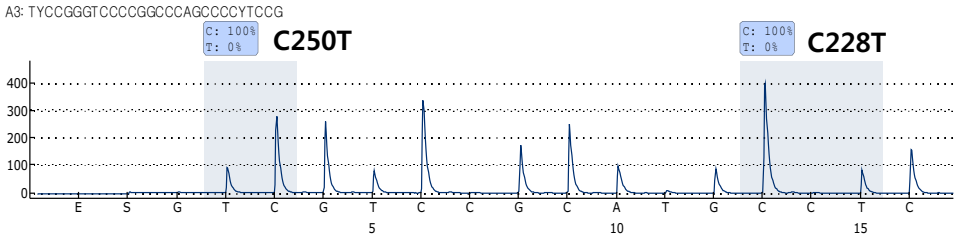

***TERT* – Positive Test**

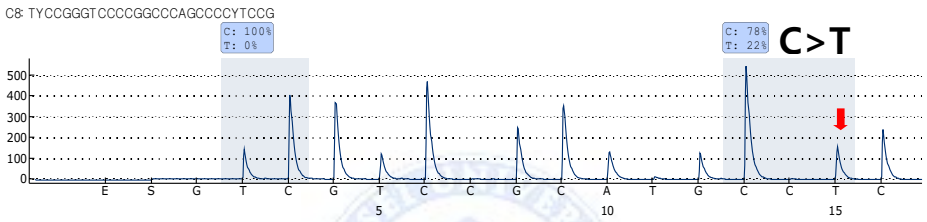

Figure 2. Results of pyrosequencing of *TERT* promoter mutation

3. Construction of tissue microarray (TMA)

For the immunohistochemical (IHC) study, TMA blocks were made using representative, well-fixed tumor samples (two cores, 2 mm in diameter) and normal tissue samples (1 core, 2 mm in diameter) from the FFPE blocks

4. Immunohistochemistry

Immunohistochemistry of samples from both PTC groups was performed using 4-μm thick FFPE tissue sections on silane-coated slides. After drying the slides in an oven for 1 hour, immunostaining was performed automatically using a Ventana BenchMark XT Autostainer (Ventana Medical Systems,

Tucson, AZ, USA) and an OptiVew DAB IHC Detection kit (Ventana Medical Systems). The protocol consisted of a 48-minute antigen-retrieval step in CC1 (Cell conditioning); a 10-minute endogenous peroxidase blocking step in peroxide block; a 16-minute incubation in 42℃ with primary antibodies, including NIS (monoclonal mouse, 1:50, Thermo, USA), TSHR (4C1/E1/E8, mouse monoclonal, 1: 100, Abcam Inc. Cambridge, MA), VEGF (C-1, mouse monoclonal, 1:200, Santa Cruz Biotechnology, Inc., Santa Cruz, CA), VEGFR2 (55B11, rabbit monoclonal, 1:200, Cell Signaling Technology, Beverly, MA), NF-κB p65 (F-6, mouse monoclonal, 1: 1000, Santa Cruz Biotechnology, INC., Santa Cruz, CA), β-catenin (β-catenin-1, mouse monoclonal, 1:100, DAKO, Carpinteria, CA) and PTEN (6H2.1, mouse monoclonal, 1: 100, Biocare Medical, Walnut Creek, CA).

5. Interpretation of immunohistochemistry

Nuclear and cytoplasmic staining for NIS and TSHR, cytoplasmic staining for NF-κB, VEGF, and PTEN, cytoplasmic staining of vascular endothelial cells for VEGFR2, and nuclear staining for β-catenin were considered positive and evaluated by light microscopy. The results of IHC staining were defined by intensity and volume. “Volume” was the proportion of stained cells and “intensity”, was classified as 0 (negative), 1 + (weak), 2+ (moderate), and 3+ (strong).

Modified scores for immunohistochemistry are reported as follows: 0, no stained cells; 1, when 1–49% of tumor cells were stained with weak intensity; 2, when ≥ 50% of tumor cells were stained with weak intensity; 3, when 1–49% of tumor cells were stained with moderate intensity; 4, when ≥ 50% of tumor cells were stained with moderate intensity; 5, 1–49% of tumor cells were stained with strong intensity; and 6, when ≥ 50% of tumor cells were stained with strong intensity. Loss of expression of PTEN was scored in reverse order.

6. Statistical analysis

Statistical analysis of data was performed using the SPSS software (version 21.0; SPSS Inc., Chicago, IL, USA). The *t* and $\chi 2$ tests were used to analyze differences between two groups for each variable. Correlation analysis was performed between variables. Logistic regression was performed to assess odds ratios (OR) and 95% confidence intervals (CI) for radioiodine-refractoriness with multiple variables including clinicopathologic features and results of mutation analysis. All *P* values were 2-sided and $P < 0.05$ was considered statistically significant.

III. RESULTS

1. Clinicopathologic characteristics of RI-refractory and RI-responsive PTCs

The RI-refractory and RI-responsive groups differed significantly in clinicopathologic features. Histologically, a significantly increased proportion of small clusters/micropapillae without fibrovascular cores (Figure 3A and 3C) and/or hobnail components were observed in both the periphery and center of tumors in RI-refractory PTCs (Figure 3C), and the maximum height/width ratio of tumor cells was ≥3 in this group (Figure 4A). Tumor necrosis and mitosis are comparatively rare in differentiated papillary carcinoma, but they were observed in RI-refractory PTCs (Figure 3E). Interestingly, the location of tumor cell nuclei in RI-refractory PTCs was mostly middle to base (Figure 4A), but apex to middle in RI-responsive PTCs (Figure 4B). RI-responsive PTCs showed occasional areas of small clusters of tumor cells or single cells at tumor peripheries; these were mostly cuboidal to columnar in appearance and the location of nuclei was middle to apical (Figure 3B and 3D). Clinicopathologically, RI-refractory PTCs showed significantly increased frequency of extrathyroidal extension of tumor and involvement of the resection margin with lymph node metastasis at initial diagnosis (Table 1).

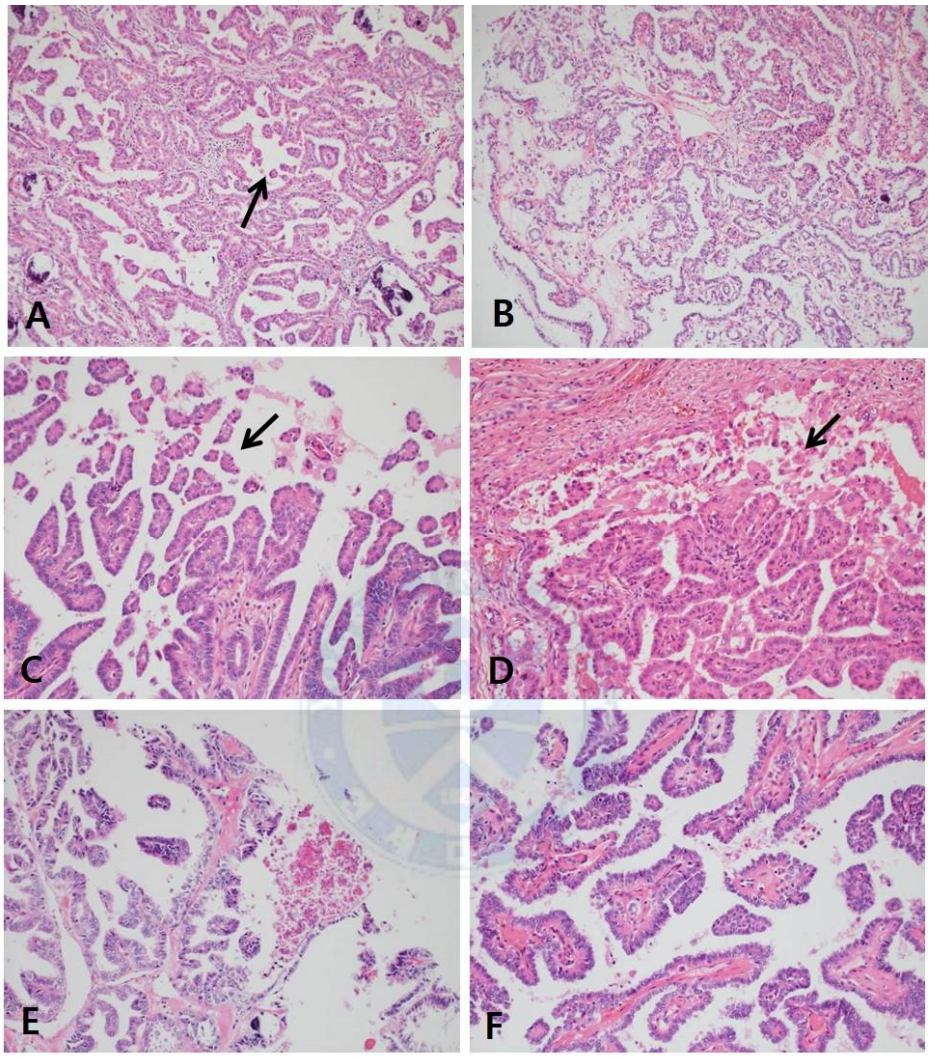

Figure 3. Representative histologic features of radioiodine-refractory papillary thyroid cancers. (A, C, E) and radioiodine-responsive papillary thyroid cancers (B, D, F). Both types of tumors show classic papillary architecture with varying degrees of small clusters/micropapillae without fibrovascular cores (arrow) or discohesive single cells. Tumor necrosis is comparatively rare, but remarkably

increased in the radioiodine-refractory group rather than the radioiodine-responsive group (E).

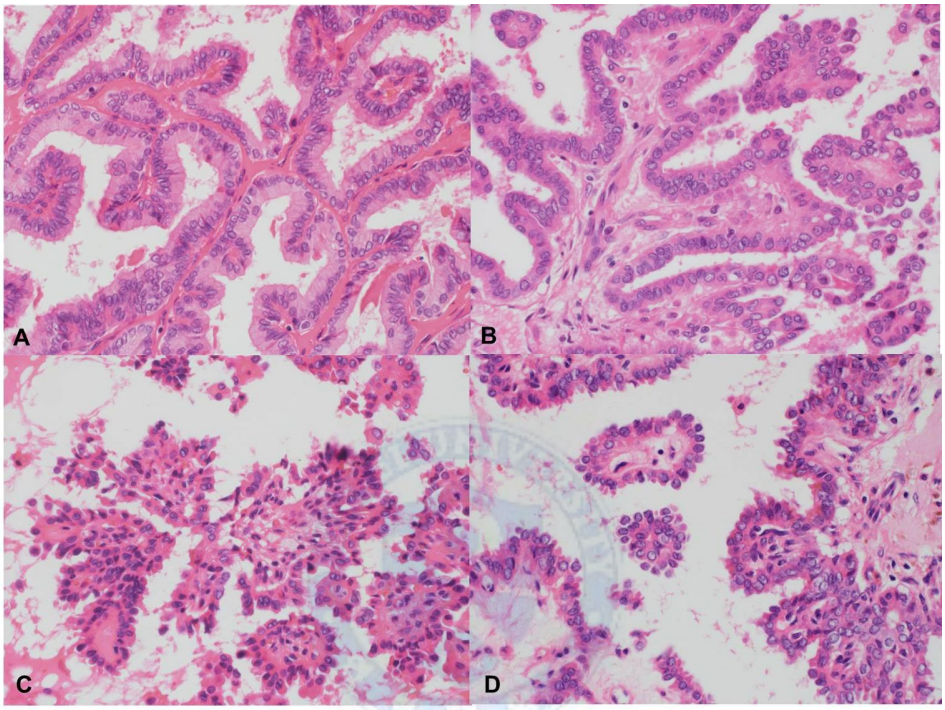

Figure 4. Histologic features of classic papillary pattern and hobnail pattern of papillary thyroid cancers (A–D). In some radioiodine-refractory cases, tumor cells have longer and more slender papillary structure, with increased height/width ratio (≥ 3) and base to middle location of nuclei (A) or a hobnail pattern, with elongated nuclei within the cell apex (C and D). Tumor cells of radioiodine-responsive cases reveal mostly cuboidal or columnar in appearance, and nuclei were located in the middle to apex of the cell (B).

Table 1. Clinicopathologic features of radioiodine-refractory and radioiodine-responsive papillary thyroid cancers

Clinicopathologic features		RI-refractory PTC (N = 26)	RI-responsive PTC (N = 82)	*P*-value
Gender (%)	Male	13 (50)	37 (45.1)	0.664
	Female	13 (50)	45 (54.9)	
Age at diagnosis	Median, yr (Range)	58 (16-71)	51 (18-71)	0.063*
Histologic type (%)	Conventional	23 (88.5)	76 (92.7)	0.231
	Diffuse-sclerosing	2 (7.7)	2 (2.4)	
	Follicular	0	3 (3.7)	
	Hurthle cell	1 (3.8)	0	
	Cribriform-morular	0	1 (1.2)	
	Tall cell	0	0	
Histologic features				
Small clusters (%)[1]	< 20%	9 (34.6)	76 (92.7)	<0.001
	≥ 20%	17 (65.4)	6 (7.3)	
Small clusters in tumor center	Absent	5 (19.2)	39 (47.6)	0.01
	Present	21 (80.8)	43 (52.4)	
Hobnail feature (%)	< 5%	5 (19.2)	46 (56.1)	0.001
	≥ 5%	21 (80.8%)	36 (43.9)	
Hobnail feature in tumor center	Absent	18(69.2)	72 (87.8)	0.036†
	Present	8 (30.8)	10 (12.2)	
Tall cell feature (%)[2]	<10%	12 (46.2)	79 (96.3)	<0.001†
	≥ 10%, < 50%	14 (53.8)	3 (3.7)	
Necrosis	Absent	10 (38.5)	81 (98.8)	<0.001†
	Present	16 (61.5)	1 (1.2)	

Clinicopathologic features		RI-refractory PTC (N = 26)	RI-responsive PTC (N = 82)	*P*-value
Height/Width ratio of tumor cell (%)	Maximum < 3	12 (46.2)	76 (92.7)	<0.001†
	Maximum ≥ 3	14 (53.8)	6 (7.3)	
Location of nuclei (%)[3]	Apex	2 (9.5)	19 (90.5)	0.013†
	Middle	22 (25.9)	63 (74.1)	0.016‡
	Base	2 (100)	0	
Mitosis	Absent	14 (53.8)	80 (97.6)	<0.001†
	Present	12 (46.2)	2 (2.4)	
Tumor multifocality	Single	9 (34.6)	46 (56.1)	0.056
	Multifocal	17 (65.4)	36 (43.9)	
Tumor size (%)	≤2 ㎝	10 (38.5)	66 (80.5)	< 0.001
	>2 ㎝, ≤4 ㎝	9 (34.6)	14 (17.1)	
	>4 ㎝	7 (26.9)	2 (2.4)	
Lymph node metastasis (%)	Absent	2 (7.7)	23 (28)	0.032
	Present	24 (92.3)	59 (72)	
Extrathyroidal extension	Absent	2 (7.7)	23 (28)	0.032
	Present	24 (92.3)	59 (75.9)	
Resection margin	Negative	17 (65.4)	80 (97.6)	<0.001†
	Positive	9 (34.6)	2 (2.4)	
Tumor margin	Expanding	1 (3.8)	18 (22.5)	0.038†
	Infiltrative	25 (96.2)	62 (77.5)	

Clinicopathologic features		RI-refractory PTC (N = 26)	RI-responsive PTC (N = 82)	*P*-value
Stage (%)	I	5	33	< 0.001
	II	1	0	
	III	3	32	
	IVA	13	17	
	IVB	1	0	
	IVC	3	0	

* Mann-Whitney test, † Fisher's exact test, ‡ Linear-by-Linear Association; [1]small tumor clusters composed of micropapillae without fibrovascular cores; [2] the tumor cells show a granular eosinophilic cytoplasm with a height is at least triple their width (< 50% of tumor); [3]The main location of nuclei within tumor cell; RI, radioiodine; PTC, papillary thyroid cancer.

2. *BRAF* V600E and *TERT* mutation results

A. Individual incidence of molecular variables in each groups

The *TERT* promoter mutation ($P < 0.001$) was found in 14/26 cases of RI-refractory PTC (53.8%, 13 *TERT* C228T, 1 *TERT* C250T) but in only 1/82 cases of RI-responsive PTC (1.2%, in *TERT* C228T). The *BRAF* V600E mutation was found in more than 80% of cases in both groups (21/26, 80.8% in the RI-refractory group and 67/82, 81.7% in the RI-responsive group) (Table 2).

Table 2. Incidences of *TERT* promoter mutations and *BRAF* V600E mutation in radioiodine-refractory and radioiodine-responsive papillary thyroid cancers

Mutation	RI-refractory PTC (N = 26)	RI-responsive PTC (N = 82)	Total (N = 108)	*P*-value*
TERT promoter (%)	14 (53.8)	1 (1.2)	15 (13.9)	<0.001
Type of Mutation				
C250T	1 (3.8)	0	1 (0.9)	0.241
C228T	13 (50)	1 (1.2)	14 (13)	<0.001
BRAF V600E (%)	21 (80.8)	67 (81.7)	88 (81.5)	1

* Fisher's exact test; RI, radioiodine; PTC, papillary thyroid cancer.

B. Combined incidence of molecular variables in each groups

Coexistence of *TERT* promoter and *BRAF* mutations was found in 13/108 (12%) in all cases of PTC, either RI-refractory or RI-responsive. Coexistence of two mutations was observed in only 1 case of RI-responsive PTC; in 18 cases, no mutation was identified (Table 3).

Table 3. Combined incidences of *TERT* promoter mutations and *BRAF* V600E mutation in radioiodine-refractory and radioiodine-responsive papillary thyroid cancers

	Total	*TERT* C228T		*TERT* C250T	
		Wild	Mutant	Wild	Mutant
RI-refractory PTC	26	13	13	25	1
BRAF-Wild	5	3	2	5	0
BRAF-Mutant	21	10	11	20	1
RI-responsive PTC	82	81	1	82	0
BRAF-Wild	15	15	0	15	0
BRAF-Mutant	67	66	1	67	0

RI, radioiodine; PTC, papillary thyroid cancer.

C. Relationship between clinicopathologic features and expressions of molecular variables

In the analysis of correlation between molecular changes and clinicopathologic features, *TERT* promoter mutations were similarly associated with clinicopathologic features including small clusters, hobnail component, height/width of tumor cells, necrosis, mitosis and resection margin; the significance of each association is reported in (Table 4).

Table 4. Relationship between **c**linicopathologic features and *TERT* promoter mutation or *BRAF* V600E mutation in papillary thyroid cancers

	TERT all mutations			*BRAF* V600E		
Total PTC (N = 108)	Wild (N = 93)	Mutant (N = 15)	*P*- value	Wild (N = 20)	Mutant (N = 88)	*P*- value
Gender (%)						
Male	45 (48.4)	5 (33.3)	0.278	7 (35)	43 (48.9)	0.262
Female	48 (51.6)	10 (66.7)		13 (65)	45 (51.1)	
Median age at diagnosis (range)	51 (17-71)	62 (16-71)	0.007*	50.5 (17-70)	52 (16-71)	0.519*
Histologic type (%)						
Conventional	85 (91.4)	14 (93.3)	0.366†	16 (80)	83 (94.3)	0.078†
Diffuse-sclerosing	4 (4.3)	0		2 (10)	2 (2.3)	
Follicular	3 (3.2)	0		1 (5)	2 (2.3)	
Hurthle cell	0	1 (6.7)		0	1 (1.1)	
Cribriform-morular	1 (1.1)	0		1 (5)	0	
Tall cell	0	0		0	0	
Histologic features						
Small clusters (%)[1]						
< 20%	81 (87.1)	4 (26.7)	<0.001†	16 (80)	69 (78.4)	1†
≥ 20%	12 (12.9)	11 (73.3)		4 (20)	19 (21.6)	
Small clusters in tumor center						
Absent	43 (46.2)	1 (6.7)	0.004	9 (45)	35 (39.8)	0.668
Present	50 (53.8)	14 (93.3)		11 (55)	53 (60.2)	

Total PTC (N = 108)	*TERT* all mutations		*P*- value	*BRAF* V600E		*P*- value
	Wild (N = 93)	Mutant (N = 15)		Wild (N = 20)	Mutant (N = 88)	
Hobnail feature (%)						
< 5%	49 (52.7)	2 (13.3)	0.005	9 (45)	42 (47.7)	0.825
≥ 5%	44 (47.3)	13 (86.7)		11 (55)	46 (52.3)	
Hobnail feature in tumor center						
Absent	82 (88.2)	8 (53.3)	0.003†	17 (85)	73 (83)	1†
Present	11 (11.8)	7 (46.7)		3 (15)	15 (17)	
Tall cell feature (%)[2]						
<10%	85 (91.4)	6 (40)	0.001†	17 (85)	74 (84.1)	1†
≥ 10%	8 (8.6)	9 (60)		3 (15)	14 (15.9)	
Height/Width ratio of tumor cell (%)						
Max. < 3	81 (87.1)	7 (46.7)	0.001†	16 (80)	72 (81.8)	1†
Max. ≥ 3	12 (12.9)	8 (53.3)		4 (20)	16 (18.2)	
Location of nuclei (%)[3]						
Apex	19 (90.5)	2 (9.5)	0.287‡	5 (23.8)	16 (76.2)	0.392‡
Middle	73 (85.9)	12 (14.1)		15 (17.6)	70 (82.4)	
Base	1 (50)	1 (50)		0	2 (100)	
Necrosis						
Absent	85 (91.4)	6 (40)	<0.001†	17 (85)	74 (84.1)	1†
Present	8 (8.6)	9 (60)		3 (15)	14 (15.9)	
Mitosis						
Absent	84 (90.3)	10 (66.7)	0.025†	17 (85)	77 (87.5)	0.721†
Present	9 (9.7)	5 (33.3)		3 (15)	11 (12.5)	

Total PTC (N = 108)	*TERT* all mutations		*P*- value	*BRAF* V600E		*P*- value
	Wild (N = 93)	Mutant (N = 15)		Wild (N = 20)	Mutant (N = 88)	
Tumor multifocality						
Single	50 (53.8)	5 (33.3)	0.142	11 (55)	44 (50)	0.686
Multifocal	43 (46.2)	10 (66.7)		9 (45)	44 (50)	
Tumor size (%)						
≤2 ㎝	72 (77.4)	4 (26.7)	<0.001†	12 (60)	64 (72.7)	0.024†
>2 ㎝, ≤4 ㎝	18 (19.4)	5 (33.3)		3 (15)	20 (22.7)	
>4 ㎝	3 (3.2)	6 (40)		5 (25)	4 (4.5)	
Lymph node metastasis (%)						
Absent	24 (25.8)	1 (6.7)	0.184†	8 (40)	17 (19.3)	0.075†
Present	69 (74.2)	14 (93.3)		12 (60)	71 (80.7)	
Extrathyroidal extension						
Absent	24 (25.8)	1 (6.7)	0.184†	5 (25)	20 (22.7)	0.777†
Present	69 (74.2)	14 (93.3)		15 (75)	68 (77.3)	
Resection margin						
Absent	87 (93.5)	10 (66.7)	0.007†	18 (90)	79 (89.8)	1†
Positive	6 (6.5)	5 (33.3)		2 (10)	9 (10.2)	
Tumor margin						
Expanding	19 (20.9)	0	0.067†	6 (30)	13 (15.1)	0.191†
Infiltrative	72 (79.1)	15 (100)		14 (70)	73 (84.9)	
Stage (%)						
I	36	2	<0.001†	8	30	0.983†
II	0	1		0	1	
III	35	1		7	29	

Total PTC (N = 108)	*TERT* all mutations		*P*- value	*BRAF* V600E		*P*- value
	Wild (N = 93)	Mutant (N = 15)		Wild (N = 20)	Mutant (N = 88)	
IVA	19	10		5	24	
IVB	1	0		0	1	
IVC	2	1		0	3	

* Mann-Whitney test; † Fisher's Exact test; ‡ Linear-by-Linear Association; [1]small tumor clusters composed of micropapillae without fibrovascular cores; [2] the tumor cells show a granular eosinophilic cytoplasm with a height is at least triple their width (< 50% of tumor); [3]The main location of nuclei within tumor cell; PTC, papillary thyroid cancer.

3. Immunohistochemical stain results

A. Individual immunohistochemical stain results in each groups

Immunohistochemically, expression of NIS and TSHR, which are involved in the MAPK pathway, was markedly decreased in many cases of RI-refractory PTC ($P < 0.05$). Expression of VEGF, VEGFR2, and NF-κB, which are known to be oncogenic proteins that are up-regulated in PTC, was somewhat lower in RI-refractory PTC than in RI-responsive PTC ($P < 0.05$). Total loss of PTEN expression was occasionally observed in both RI-refractory PTC (26.9%) and RI-responsive PTC (15.9%). β-catenin, which is involved in the WNT-β-catenin pathway, showed cytoplasmic positive reactivity in all PTCs (Table 5).

Table 5. Individual immunohistochemical stain results in radioiodine-refractory and radioiodine-responsive papillary thyroid cancers

Immunohistochemistry (N = 108)		RI-refractory PTC (N = 26)	RI-responsive PTC (N = 82)	*P*-value
NIS	<1+, 50%	12 (46.2)	21 (25.6)	0.048
	≥1+, 50%	14 (53.8)	61 (74.4)	
TSHR	<2+	17 (65.4)	21 (25.6)	0.000
	≥2+	9 (34.6)	61 (74.4)	
VEGF	<3+, 50%	17 (65.4)	32 (39%)	0.019
	≥3+, 50%	9 (34.6)	50 (61%)	
VEGFR2	<2+*	11 (42.3)	16 (19.5)	0.019
	≥2+	15 (57.7)	66 (80.5)	
NF-κB	<1+, 50%	9 (34.6)	11 (13.4)	0.022†
	≥1+, 50%	17 (65.4)	71 (86.6)	
PTEN	negative	7 (26.9)	13 (15.9)	0.248†
	positive	19 (73.1)	69 (84.1)	

† Fisher's exact test; Chi-squared test: not annotated; intensity of immunehisto chemical staining: 0, 1+, 2+, 3+, *2+: ≥ 30% in stroma; RI, radioiodine; PTC, papillary thyroid cancer; NIS, sodium iodide symporter; TSHR, thyroglobulin stimulating hormone receptor; VEGF, vascular endothelial cell growth factor; VEGFR2, vascular endothelial cell growth factor receptor 2; NF-κB, nuclear factor kappa-light-chain-enhancer of activated B cells.

B. Relationship between immunohistochemical results and expressions of molecular variables

Comparative analysis of immunohistochemical results with *TERT* and *BRAF* mutations in all PTC revealed no correlation with *TERT* and *BRAF* mutation status, except for TSHR ($P = 0.03$, *TERT* mutation) in all PTC (Table 6).

C. Relationship between clinicopathologic features and immunohisto chemical results

In Spearman correlation analysis between immunohistochemical and histopathologic features, negative correlations were observed between NIS and small clusters ($r = -0.212$, $P = 0.027$), NIS and hobnail features ($r = -0.249$, $P = 0.009$), TSHR and height/width of tumor cells ($r = -0.279$, $P = 0.003$), PTEN and small cluster in tumor centers ($r = -0.232$, $P = 0.016$), VEGFR2 and small clusters ($r = -0.272$, $P = 0.004$), VEGFR2 and small clusters in tumor centers ($r = -0.308$, $P = 0.001$), and VEGF and hobnail features in tumor centers ($r = -0.197$, $P = 0.042$). Positive intercorrelations were observed between VEGF and NF-κB ($r = 0.252$, $P = 0.009$), hobnail features and hobnail features in tumor centers ($r = 0.550$, $P < 0.001$), hobnail features and small clusters ($r = 0.662$, $P < 0.001$), hobnail features and small clusters in tumor centers ($r = 0.537$, $P < 0.001$), small clusters and height/width of tumor cells ($r = 0.351$, $P < 0.001$), small clusters in tumor centers and height/width of tumor cells ($r = 0.247$, $P =$

0.010). The Mann-Whitney test and Fisher's exact test confirmed the significance of these results. Significant associations between histologic features and immunohistochemical results were observed in the RI-refractory and RI-responsive groups (Figure 5).

4. Combined utility of variables for predicting radioiodine-refractoriness

Prior to conducting the logistic regression analysis of RI-refractoriness in PTC, the sensitivity and specificity for predicting RI-refractory PTC were calculated. Among the sixteen variables, presence of necrosis and *TERT* mutation had high specificity (99%) and high accuracy (89.8% and 88%, respectively). Small clusters (≥10%), small clusters in tumor centers, and hobnail features had high sensitivity (88%, 81%, and 81%, respectively). Combined with other variables, especially with necrosis, both sensitivity and specificity increased. Other sets of variables, such as presence of *TERT* mutation or mitosis, were also analyzed, but no significant associations were observed (Table 7).

In the logistic regression analysis, fourteen variables were incorporated, and useful predictors of RI-refractoriness were selected by likelihood ratio, using a backward stepwise method. Four features that can be used to predict of RI-refractoriness were identified: *TERT* mutation, height/width of tumor cells ≥ 3, increased small clusters (≥ 20%), and necrosis (Table 8).

Table 6. Relationship between immunohistochemical results and expressions of mutations of *TERT* and *BRAF* V600E

Immunohistochemistry		*TERT* all mutations			*BRAF* V600E		
		Wild	Mutant		Wild	Mutant	
	(N = 108)	(N = 93)	(N = 15)	P- value	(N = 20)	(N = 88)	P-value
NIS	<1+, 50%	26 (28)	7 (46.7)	0.225†	8 (40)	25 (28.4)	0.310
	≥1+, 50%	67 (72)	8 (53.3)		12 (60)	63 (71.6)	
TSHR	<2+	29 (31.2)	9 (60)	0.030	9 (45)	29 (33)	0.309
	≥2+	64 (68.8)	6 (40)		11 (55)	59 (67)	
VEGF	< 3+	32 (34.4)	6 (40)	0.674	10 (50)	28 (31.8)	0.124
	≥3+	61 (65.6)	9 (60)		10 (50)	60 (68.2)	
VEGFR2	<2+*	21 (22.6)	6 (40)	0.197†	4 (20)	23 (26.1)	0.567
	≥2+	72 (77.4)	9 (60)		16 (80)	65 (73.9)	
NF-κB	<3+, 50%	53 (57)	10 (66.7)	0.481	16 (80)	47 (53.4)	0.029
	≥3+, 50%	40 (43)	5 (33.3)		4 (20)	41 (46.6)	
PTEN	Negative	16 (17.2)	4 (26.7)	0.472†	6 (30)	14 (15.9)	0.199†
	Positive	77 (82.8)	11 (73.3)		14 (70)	74 (84.1)	

† Fisher's exact test, Chi-squared test: not annotated; intensity of immunohisto chemistry: 0, 1+, 2+, 3+, *2+: ≥ 30% in stroma; NIS, sodium iodide symporter; TSHR, thyroglobulin stimulating hormone receptor; VEGF, vascular endothelial cell growth factor; VEGFR2, vascular endothelial cell growth factor receptor 2; NF-κB, nuclear factor kappa-light-chain-enhancer of activated B cells.

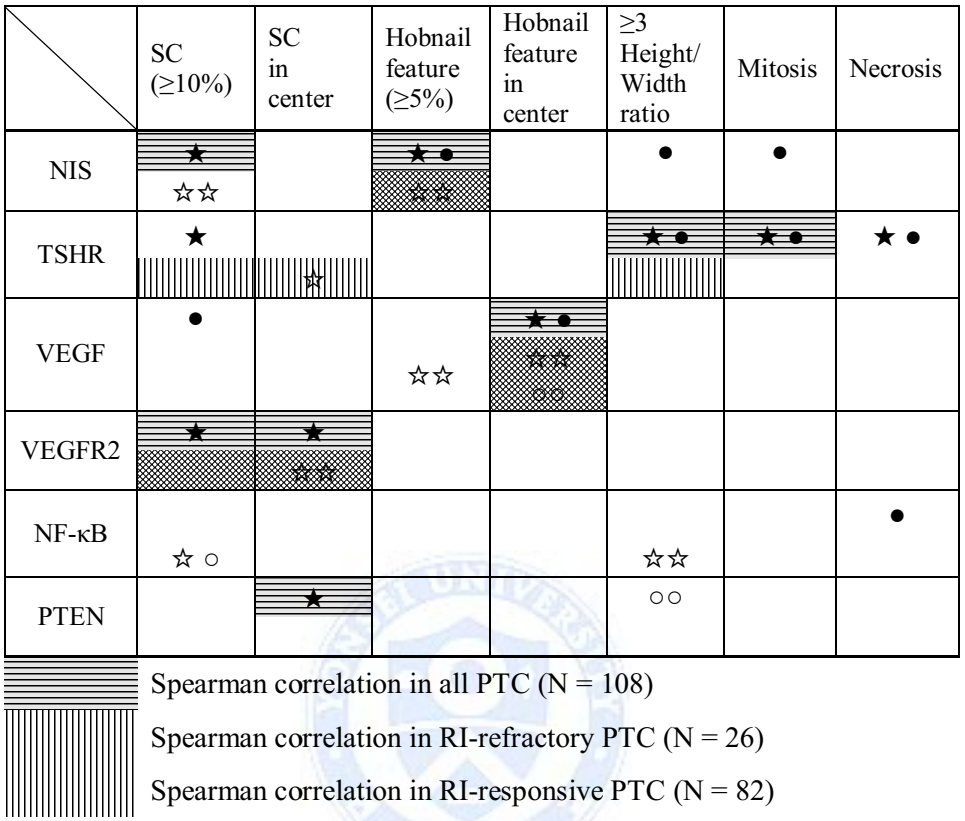

Figure 5. Relationship between clinicopathologic features and immunohisto chemical results (★Mann-Whitney test in all papillary thyroid cancers (PTC); ☆Mann-Whitney test in radioiodine refractory PTC; ☆☆Mann-Whitney test in radioiodine responsive PTC; ●Fisher's exact test or Chi-squared test in all PTC; ○Fisher's Exact test or Chi-squared test in radioiodine refractory PTC; ○○Fisher's exact test or Chi-squared test in radioiodine responsive PTC; Immunohistochemistry score, -:0, 1+: 1–2 (≥ 50%), 2+: 3–4 (≥ 50%), 3+: 5–6 (≥ 50%), cut–off value: NIS (<1+, 50%), TSHR (< 2+), VEGF (< 3+), VEGFR2 (< 2+), NF-κB (< 3+, 50%), PTEN (negative); SC, small tumor clusters composed of micropapillae without fibrovascular cores; NIS, sodium iodide symporter; TSHR, thyroglobulin stimulating hormone receptor; VEGF, vascular endothelial cell growth factor; VEGFR2, vascular endothelial cell growth factor receptor 2; NF-κB, nuclear factor kappa-light-chain-enhancer of activated B cells.)

Table 7. Sensitivity and specificity of histopathologic features and mutation in radioiodine-refractory papillary thyroid cancers

Histopathologic features	Sensitivity (%)	Specificity (%)	Accuracy (%)
Necrosis	62	99	89.8
TERT mutation	54	99	88.0
Small clusters (≥ 20%)[1]	65	93	86.1
Mitosis	46	98	85.2
Tall cell feature (≥ 10%, < 50%)[2]	54	96	86.1
Height/Width ratio in tumor cells (maximum ≥ 3)	54	93	83.3
Small clusters (≥ 10%)	88	71	75.0
NF-kB (< 1+, 50%)	35	87	74.1
Hobnail feature in center	31	88	74.1
TSHR (< 2+)	65	74	72.2
VEGFR2 (< 2+)	42	80	71.3
PTEN (Negative)	27	84	70.4
NIS (< 1, 50%)	46	74	67.6
Hobnail feature	81	56	62.0
VEGF (< 3+, 50%)	65	61	62.0
Small clusters in center	81	48	55.6
BRAF V600E mutation	77	18	32.4
Necrosis + *TERT* mutation	81	98	93.5
TERT mutation + Mitosis	81	96	92.6
Necrosis + Mitosis	77	96	91.7
Necrosis + H/W3	88	91	90.7
Mitosis + SC20	85	90	88.9
TERT mutation + H/W3	77	91	88.0
Necrosis + SC20	77	91	88.0

Histopathologic features	Sensitivity (%)	Specificity (%)	Accuracy (%)
H/W3 + SC20	92	85	87.0
Necrosis + Mitosis + *TERT* mutation	96	88	89.8
TERT mutation + H/W3 + Necrosis + Mitosis	96	88	89.8
TERT mutation + H/W3 + Necrosis + SC20	96	83	86.1
TERT mutation + H/W3 + Necrosis + SC20 + Mitosis	100	80	85.2
TERT mutation + H/W3 + SC10 + TSHR + NFKB	100	43	56.5
TERT mutation + SC10 + TSHR + NFKB	100	46	59.3

[1]small tumor clusters composed of micropapillae without fibrovascular cores; [2] the tumor cells show a granular eosinophilic cytoplasm with a height is at least triple their width (< 50% of tumor); NF-κB, nuclear factor kappa-light -chain-enhancer of activated B cells; TSHR, thyroglobulin stimulating hormone receptor; VEGFR2, vascular endothelial cell growth factor receptor 2; VEGF, vascular endothelial cell growth factor; NIS, sodium iodide symporter; H/W3, height//width ratio in tumor cells (maximum ≥ 3); SC20, small clusters (≥ 20%); SC10, small clusters (≥ 10%).

Table 8. Logistic regression analysis on radioiodine-refractoriness in papillary thyroid cancers (N = 108)

Variables	B	S.E	p-value	Odd Ratio	95% C.I
Univariate regression					
Small clusters (≥ 20%)	3.175	0.591	< 0.001	23.926	7.51-76.26
Small clusters (≥ 10%)	2.919	0.660	< 0.001	18.528	5.08-67.56
Small clusters in center	1.337	0.545	0.014	3.809	1.31-11.08
Hobnail feature (≥ 5%)	1.680	0.545	0.002	5.367	1.84-15.62
Hobnail features in center	1.163	0.543	0.032	3.200	1.11-9.27
Tall cell feature (≥ 10%)	1.885	0.310	< 0.001	6.583	0.008-0.130
Necrosis (present)	4.864	1.084	< 0.001	129.6	15.49-1084.489
Mitosis (≥ 1/10HPF)	3.535	0.817	< 0.001	34.286	6.92-169.99
Height/Width ratio of tumor cell (maximum ≥ 3)	2.693	0.578	< 0.001	14.778	4.56-45.92
TERT mutation	4.549	1.080	< 0.001	94.5	11.37-785.25
BRAF V600E mutation	-0.062	0.574	0.915	0.940	0.31-2.90
NIS (< 1+, 50%)	0.912	0.486	0.051	2.490	0.99-6.23
TSHR (< 2+)	1.702	0.484	<0.001	5.487	2.13-14.16
VEGF (< 3+)	1.082	0.470	0.021	2.951	1.17-7.42
VEGFR2 (< 2+)	1.107	0.485	0.022	3.025	1.17-7.83

Variables	B	S.E	p-value	Odd Ratio	95% C.I
NF-κB (< 1+, 50%)	1.229	0.5245	0.019	0.293	0.105-0.818
PTEN (negative)	0.671	0.536	0.211	1.955	0.68-5.59
Multivariate regression (stepwise selection)					
Constant	-7.854	2.517	0.002	0.000	
TERT mutation	4.07	1.859	0.029	58.529	1.532-2235.634
Height/Width ratio of tumor cell (maximum ≥ 3)	3.717	1.481	0.012	41.143	2.259-749.405
Small clusters (≥ 20%)	4.049	1.608	0.012	57.315	2.451-1340.483
Necrosis	5.407	1.862	0.004	223.067	5.803-8574.022
TSHR (<2+)	2.870	1.569	0.067	17.629	0.815-381.453
VEGFR2 (<2+)	2.617	1.553	0.092	13.692	0.653-287.180

Logistic regression analysis was performed in radioiodine-refractory (N = 26) and radioiodine-responsive (N = 82) cases of PTC, using all available features. CI, confidence intervals; [1]small tumor clusters composed of micropapillae without fibrovascular cores; [2] the tumor cells show a granular eosinophilic cytoplasm with a height is at least triple their width (< 50% of tumor); NIS, sodium iodide symporter; TSHR, thyroglobulin stimulating hormone receptor; VEGF, vascular endothelial cell growth factor; VEGFR2, vascular endothelial cell growth factor receptor 2; NF-κB, nuclear factor kappa-light-chain-enhancer of activated B cells.

IV. DISCUSSION

In this study, we find out that an increased frequency of small clusters or hobnail features in tumors and the presence of small clusters or hobnail features especially in tumor centers were significant predictor of RI-refractoriness in PTCs.

The prognosis for PTCs is generally favorable. However, some variants of PTCs, including the tall cell, columnar, diffuse sclerosing, and solid variants, are associated with more aggressive clinical features. [46] A recently described, new variant of PTC exhibiting > 30% micropapillary or hobnail feature in tumor cells demonstrates discohesive growth and single cells with a loss of polarity. In this variant, nuclei show characteristic apical placement and bulging out to surface.[47,48] This rare hobnail variant is associated with a higher mortality rate than classic PTC, and is associated with frequent lymph node metastasis, recurrence, and distant metastasis.[48] A recent study reported that PTC can be considered to have hobnail features if the hobnail component comprises at least 10% of the tumor. Although the proportion of hobnail or small clusters is lower than 30% of PTC, it is significantly associated with poor prognosis. In one case study, small clusters or a hobnail component were most often found especially at the tumor-infiltrating edge or periphery.[48] Similarly, in this study, the frequency of small clusters or hobnail features in tumors and the presence of small clusters or hobnail features in tumor centers were significantly higher in

RI-refractory PTC than in RI-responsive PTCs.

Additionally, we suggest that an increased maximum height/width ratio in tumor cells (≥3) in non-tall cell variant PTC could predict RI-refractoriness.

The tall cell variant of PTC also shows aggressive behavior, similar to the hobnail variant. Histologically, ≥50% of the tumor cells show a granular eosinophilic cytoplasm with a height is at least triple their width. However, in recent case studies, a ≥10% cut−off threshold for tall cell quantity has been suggested to be strongly associated with a poorer clinical outcome.[49] Here, we showed that a higher (≥3) maximum height/width ratio of tumor cells in the non-tall cell variant of PTCs was were significantly associated with RI-refractory PTC and predict of RI-refractoriness. These data support its use as a prognostic factor of aggression in PTC. *TERT* promoter mutations in the tall cell variant have recently been found to be a strong predictor of tumor relapse.[37-39] *TERT* promoter mutation and maximum height/width ratio of tumor cells (≥3) were also found to be significantly associated in this study.

Immunohistochemically, the decreased expression of NIS and TSHR observed in this study suggests that impairment of the iodide-handling machinery, and it may be associated with RI refractoriness.

Transportation of iodide through the sodium–iodide symporter (NIS) is up-regulated by TSH-mediated activation of TSHR.[26] In previous studies, NIS

protein was found to be expressed in the cytoplasm rather than the cytoplasmic membrane of cancer cells,[50] and the intracellular expression of NIS protein might be related to its inactivation, due to intracellular migration.[51] In this study, the NIS protein was expressed mostly in the intranuclear portion of tumor cells, but it was strongly expressed in the intracellular or basolateral membrane in normal follicular cells. No staining was observed in the lung or liver tissue used as negative controls. According to a recent study of expression of NIS in different PTC variants, strong intranuclear or nuclear membrane staining for NIS protein was observed in conventional PTCs, and staining for NIS protein was negative (0 and 1+) in the tall cell and diffuse sclerosing variants of PTC, which are considered to be aggressive subtypes of PTC.[31] In advanced thyroid cancers, failure of RI treatment may be associated with impairment of the iodide- handling machinery.[9] Similarly, we observed the decreased expression of NIS and TSHR in RI-refractory PTC, and we suggest that impairment of the iodide-handling machinery may be associated with RI refractoriness.

The aggressive behavior of *TERT*-mutated tumors may be associated with the alteration of function of NIS and other genes, which leads to decreased RI avidity and failure of RI treatment. According to our results, impairment of NIS expression was correlated with *TERT* promoter mutation, but not with *BRAF* V600E mutation. Concordant with our results, *TERT* promoter mutation was considered to be an independent predictor of distant metastases and disease

progression in DTC.[36]

The impairment of the iodide-handling machinery may be associated with aberrant activation of the MAPK signaling pathway, especially in mutation of *BRAF* V600E, which was found to be associated with RI refractoriness in previous studies. [16,28-30] Although the expression of NIS protein was not correlated with *BRAF* V600E mutation in this study, overall observation of whole tumor sections may be required to observed this association, because of the heterogeneous expression of NIS in PTC and metastatic lymph nodes.[28]

The impairment of the iodide-handling machinery may also be associated with activation of the PI3K–AKT signaling pathway in human thyroid cancer cells.[32] Although PTEN loss did not differ significantly between RI-refractory and RI-responsive PTC, further study of a large number of cases, with overall observation of whole tumor sections and evaluation of phosphorylated Akt expression may be require to determine this association.

The WNT-β-catenin pathway plays a well-established role in the regulation of cell growth and proliferation. Up-regulated β-catenin is translocated into the nucleus where it triggers transcription of various tumor-promoting genes. Up-regulation of β-catenin has been found in 66% of anaplastic thyroid cancers and 25% of poorly differentiated cancers. The WNT–β-catenin pathway play an important role in determining the aggressiveness of thyroid tumors. [25] However, the expression of β-catenin was restricted to the cytoplasm of all cases of PTC

observed in this study. This result supports the finding that activation of the WNT–β-catenin pathway is not observed in DTCs and is not associated with aggressiveness.

Experimental and clinical studies of the relationship between VEGF in endothelial cells and *TERT* mutation have shown, that vascular degeneration is associated with down-regulation of *TERT* mRNA expression. Most studies reported that *TERT* plays an important role in VEGF-mediated angiogenesis, and *TERT* may act as a VEGF transcription factor.[49] However, our study showed no significant association between *TERT* promoter mutation and expression of VEGF and VEGFR2. Although no significant associations were observed, the expression of VEGF in tumor cells was remarkably negative within the small clusters and faint in the hobnail components. These results suggest that it may be a clue to explaining the relationship between low expression of NIS and TSHR and the increased proportion of small clusters or hobnail components in RI-refractory PTC.

Among the up-regulated oncogenic proteins, NF-κB has been revealed to play an important role in controlling proliferative activity and anti-apoptotic signaling pathways in thyroid cancer cells. In recent studies, NF-κB has been shown to play a major role in cell survival via synergic cross-talk with other oncogenic signaling pathways. Up-regulation of NF-κB has been shown to be associated with *BRAF* V600E mutation.[22] Although the expression of NF-κB

was variably positive in both RI-refractory and RI-responsive PTCs, it was significantly lower in RI-refractory PTC than in RI-responsive PTC, in this study.

Coexistence of the *BRAF* V600E and *TERT* C228T mutations was identified in the most aggressive subgroup of PTC; the combination was more significantly associated with the aggressive subgroup than either mutation alone.[37] Our results also indicated that coexistence of the *BRAF* V600E and *TERT* mutations is significantly prevalent in RI-refractory PTC.

V. CONCLUSION

The following histopathologic features are characteristic of RI-refractory PTC: small tumor clusters or hobnail features in both the center and periphery of tumors, as well as tumor necrosis and increased frequency of *TERT* mutation. These features may help in predicting RI-refractoriness at diagnosis of PTC. Although it is difficult to formalize the results of multivariate logistic regression, our results suggest that these characteristic histologic features and *TERT* mutation may play a critical role in diagnostic differentiation of PTCs and prediction of RI-refractoriness.

REFERENCES

1. Ministry of Health and Welfare. 2010 Annual report of cancer statistics in Korea. Seoul: Ministry of Health and Welfare; 2012.
2. Chen AY, Jemal A, Ward EM. Increasing incidence of differentiated thyroid cancer in the United States, 1988-2005. Cancer 2009;115:3801-7.
3. Cooper DS, Doherty GM, Haugen BR, Kloos RT, Lee SL, Mandel SJ, et al. Revised American Thyroid Association management guidelines for patients with thyroid nodules and differentiated thyroid cancer. Thyroid 2009;19:1167-214.
4. Darrouzet E, Lindenthal S, Marcellin D, Pellequer JL, Pourcher T. The sodium/iodide symporter: State of the art of its molecular characterization. Biochimica et Biophysica Acta 1838 (2014) 244-53.
5. Eskandari S, Loo DDF, Dai G, Levy O, Wright EM, Carrasco N. Thyroid Na+/I− symporter: mechanism, stoichiometry, and specificity. J Biol Chem 1997;272:2723-8.
6. Mian C, Barollo S, Pennelli G, Pavan N, Rugge M, Pelizzo MR, et al. Molecular characteristics in papillary thyroid cancers with no 131 I uptake. Clin Endocrinol 2008;68:108-16.
7. Eustatia-Rutten CF, Corssmit EP, Biermasz NR, Pereira AM, Romijn JA, Smit JW. Survival and death causes in differentiated thyroid carcinoma. J

Clin Endocrinol Metab 2006;91:313-9.

8. Durante C, Haddy N, Baudin E, Leboulleux S, Hartl D, Travagli JP, et al. Long-term outcome of 444 patients with distant metastases from papillary and follicular thyroid carcinoma: benefits and limits of radioiodine therapy. J Clin Endocrinol Metab 2006;91:2892-9.
9. Omur O, Baran Y. An update on molecular biology of thyroid cancers. Crit Rev Oncol Hematol 2014;90:233-52.
10. Kojic KL, Kojic SL, Wiseman SM. Differentiated thyroid cancers: a comprehensive review of novel targeted therapies. Exper Rev Anticancer Ther 2012;12: 345-57.
11. Xing. M. Molecular pathogenesis and mechanism of thyroid cancer. Nat Rev Cancer 2013;13:184-99.
12. Kimura ET, Nikiforova MN, Zhu Z Knauf JA, Nikiforov YE, Fagin JA. High prevalence of *BRAF* mutations in thyroid cancer: genetic evidence for constitutive activation of the RET/PTC-RAS-BRAF signaling pathway in papillary thyroid carcinoma. Cancer research 2003;63:1454-7.
13. Soares P, Trovisco V, Rocha AS, Lima J, Castro P, Preto A, et al. *BRAF* mutations and *RET/PTC* rearrangements are alternative events in the etiopathogenesis of PTC. Oncogene 2003;22:4578-80.
14. Frattini M, Ferrario C, Bressan P, Balestra D, De Cecco L, Mondellini P, et al. Alternative mutations of *BRAF*, *RET* and *NTRK1* are associated with

similar but distinct gene expression patterns in papillary thyroid cancer. Oncogene 2004;23:7436-40.

15. Rahman MA, Salajegheh A, Smith RA, Lam AK. B-Raf mutation: a key player in molecular biology of cancer. Exp Mol Pathol 2013;95: 336-42.
16. Xing M. *BRAF* mutation in papillary thyroid cancer: pathogenic role, molecular bases, and clinical implications. Endocr Rev 2007;28: 742-62.
17. Legakis I, Syrigos K. Recent advances in molecular diagnosis of thyroid cancer. J Thyroid Res 2011;1-8.
18. Xing M. Genetic alterations in the phosphatidylinositol 3 kinase/Akt pathway in thyroid cancer. Thyroid 2010;20:697-706.
19. Hou P, Liu D, Shan Y, Hu S, Studeman K, Condouris S, et al. Genetic alterations and their relationship in the hosphatidylinositol 3-kinase/Akt pathway in thyroid cancer. Clin Cancer Res 2007;13:1161-70.
20. Hou P, Liu D, Xing M. Genome-wide alterations in gene methylation by the *BRAF* V600E mutation in papillary thyroid cancer cells. Endocr Relat Cancer 2007;18:687-97.
21. Pacifico F, Leonardi A. Role of NF-kappaB in thyroid cancer. Mol Cell Endocrinol 2010 28;321:29-35.
22. Li X, Abdel-Mageed AB, Mondal D, Kandil E. The nuclear factor kappa-B signaling pathway as a therapeutic target against thyroid cancers. Thyroid 2013;23:209-18.

23. Sipos JA, Shah MH. Thyroid cancer: emerging role for targeted therapies. Ther Adv Med Oncol 2010;2:3-16.

24. Soh EY, Eigelberger MS, Kim KJ, Wong MG, Young DM, Clark OH, et al. Neutralizing vascular endothelial growth factor activity inhibits thyroid cancer growth in vivo. Surgery 2000;128:1059-65;discussion 1065−6.

25. Miyake N, Maeta H, Horie S, Kitamura Y, Nanba E, Kobayashi K, et al. Absence of mutations in the beta-catenin and adenomatous polyposis coli genes in papillary and follicular thyroid carcinomas. Pathol Int 2001;51:680-5.

26. Ricarte-Filho, J. C. Rivera M, Heguy A, Ladanyi M, et al. Mutational profile of advanced primary and metastatic radioactive iodine refractory thyroid cancers reveals distinct pathogenetic roles for *BRAF*, *PIK3CA*, and *AKT1*. Cancer Res 2009;69:4885-93.

27. Xing, M. *BRAF* mutation in thyroid cancer. Endocr. Relat. Cancer 2005; 12: 245-62.

28. So YK, Son YI, Baek CH, Jeong HS, Chung MK, Ko YH. Expression of sodium-iodide symporter and TSH receptor in subclinical metastatic lymph nodes of papillary thyroid microcarcinoma. Ann Surg Oncol 2012;19:990-5.

29. Durante C, Morisi R, Moretti S, Bruno R, et al. *BRAF* mutations in papillary thyroid carcinomas inhibit genes involved in iodine metabolism. J Clin Endocrinol Metab 2007; 92:2840-3.

30. Liu D, Hu S, Hou P, Jiang D, Condouris S, Xing M. Suppression of BRAF/MEK/MAP kinase pathway restores expression of iodide-metabolizing genes in thyroid cells expressing the V600E *BRAF* mutant. Clin Cancer Res 2007; 13: 1341-49.

31. Wei S, Gao M, Zhao C, Pan Y, Li H, Li J, et al. Low expression of sodium iodide symporter expression in aggressive variants of papillary thyroid carcinoma. Int J Clin Oncol 2014;19:800-4.

32. Kogai T, Sajid-Crockett, S, Newmarch, L S, Liu YY, Brent GA. Phosphoinositide-3-kinase inhibition induces sodium/iodide symporter expression in rat thyroid cells and human papillary thyroid cancer cells. J Endocrinol 2008; 199: 243-52.

33. Liu T, Wang N, Cao J, Sofiadis A, Dinets A, Zedenius J, Sofiadis A, Dinets A, Zedenius J, et al. The age- and shorter telomere- dependent TERT promoter mutation in follicular thyroid cell-derived carcinomas. Oncogene 2014 Oct 16;33:4978-84

34. Liu X, Qu S, Liu R, Pai S, Liu D, Murugan AK, et al. Highly prevalent *TERT* promoter mutations in aggressive thyroid cancers. Endocr Relat Cancer 2013;20:603-10.

35. Xing M, Liu R. Diagnostic and prognostic *TERT* promoter mutations in thyroid fine-needle aspiration biopsy. Endocrine-Related Cancer 2014;21:825-30.

36. Vinagre J, Pinto V, Celestino R, Reis M, Pópulo H, Boaventura P, et al. Telomerase promoter mutations in cancer: an emerging molecular biomarker? Virchow's Arch 2014; 465(2): 119-33.

37. Xing M, Liu R, Murugan AK, Murugan AK, Zhu G, Zeiger MA, et.al. *BRAF* V600E and *TERT* promoter mutations cooperatively identify the most aggressive papillary thyroid cancer with highest recurrence. J Clin Oncol 2014; 32: 2718-26.

38. Liu X, Qu S, Liu R, Sheng C, Shi X, Zhu G, Sheng C, Shi X, Zhu G, et al. *TERT* promoter mutations and their association with *BRAF* V600E mutation and aggressive clinicopathological characteristics of thyroid cancer. J Clin Endocrinol Metab 2014;99:1130-6.

39. Gandofi G, Ragazzi M, Frasoldati A, Piana S, Ciarrocchi A, Sancisi A. *TERT* promoter mutations are associated with distant metastasis in papillary thyroid carcinoma. Eur J. Endocrinol 2015; 172:403-13.

40. Gessi M, van de Nes J, Griewank K, Barresi V, Buckland ME, Kirfel J, et al. Absence of *TERT* promoter mutations in primary melanocytic tumours of the central nervous system. Neuropathol Appl Neurobiol 2014;40:794-7.

41. Shi X, Liu R, Qu S, Zhu G, Bishop J, Liu X, et al. Association of *TERT* promoter mutation 1,295,228C>T with *BRAF* V600E mutation, older patient age, and distant metastasis in anaplastic thyroid cancer. J CLin Endocrinol Metab 2015;100:E632-7.

42. Wong KP, Brian HL. New molecular targeted therapy and redifferentiation therapy for radioiodine-refractory advanced papillary thyroid carcinoma: Literature Review. J Thyroid Res 2012; 2012: 818204.

43. De Lellis RA, Lloud RV, Heitz PU, Eng C. World Health Organization Classification of Tumors. Pathology and genetics of tumors of endocrine organs. 1st ed. Lyon, France: IARC Press; 2004.

44. Edge SB BD, Compton CC, Fritz AG. AJCC Cancer Staging Manual. 7th ed. New York: Springer; 2010.

45. Kim YH, Choi SE, Yoon SO, Hong SW. A testing algorithm for detection of the B-type Raf kinase V600E mutation in papillary thyroid carcinoma. Hum Pathol 2014;45:1483-8.

46. Asioli S, Erickson LA, Sebo TJ, Zhang J, Jin L, Thompson GB and Lloyd RV. Papillary thyroid carcinoma with prominent hobnail features: a new aggressive variant of moderately differentiated papillary carcinoma. A clinicopathologic, immunohistochemical and molecular study of eight cases. Am J Surg Pathol 2010; 34: 44-52.

47. Asioli S, Erickson LA, Righi A, Lloyd RV. Papillary thyroid carcinoma with hobnail features: histopathologic criteria to predict aggressive behavior. Hum Pathol 2013;44:320-8.

48. Amacher AM, Goyal B, Lewis, JS, El-Mofty SK, Chernock RD. Prevalence of a hobnail pattern in papillary, poorly differentiated, and anaplastic

thyroid carcinoma. Am J Surg Pathol 2015;39:260-5.

49. Oh WJ, Lee YS, Cho U, Bae JS, Lee S, Kim MH et al. Classic papillary thyroid carcinoma with tall cell features and tall cell variant have similar clinicopathologic features. Korean J Pathol 2014:48;201-8.

50. Hartwig FP, Nedel F, Collares TV, Tarquinio SB, Nör JE, Demarco FF. Telomeres and tissue engineering: the potential roles of *TERT* in VEGF-mediated angiogenesis. Stem Cell Rev 2012;8:1275-81.

51. Sodré AK, Rubio IG, Galrão AL, Knobel M, Tomimori EK, Alves VA, et al. Association of low sodium–iodide symporter messenger ribonucleic acid expression in malignant thyroid nodules with increased intracellular protein staining. J Clin Endocrinol Metab 2008;93:4141-5.

ABSTRACT (IN KOREAN)

갑상선 유두암에서 방사성요오드 치료 내성군의 유전자변이 및 조직학적 특징

<지도교수 홍 순 원 >

연세대학교 대학원 의학과

표 주 연

갑상선의 가장 흔한 악성 종양인 유두암은 최근 현저히 발생률이 증가하고 있지만 표준치료인 수술적 치료와 방사성 요오드 치료 및 갑상선 자극호르몬의 억제치료에 잘 반응한다. 하지만 유두암 중 일부는 표준치료 후에도 재발하거나 원격 전이를 보이며 방사성요오드에 섭취가 안 되는 방사성요오드 치료 내성군으로 빠르게 진행하며, 이들 중에서는 미분화 갑상선암으로의 역분화를 보이기도 한다. 최근 갑상선암의 발생과 진행과 관련하여 분자생물학적인 연구의 비약적인 발전이 있어왔고, 가장 최근에는 염색체 끝분절(telomere)의 끝분절효소(telomerase)의 구성 요소인 역전사 요소(telomerase reverse transcriptase catalytic subunit, *TERT*)의 발현이 끝분절효소의 활성과 관련되어 있는 것이 보고되었다. *TERT* promoter의 돌연변이가 확인되어 분화갑상선암에서보다 미분화 갑상선암에서 현저히 증가된다는 보고가 있었으며, *BRAF* V600E와 *TERT* C228T 돌연변이가 함께 있는 경우에는 따로 관여할 때보다 암의 재발율이 현저히 증가하며 암의 공격적인 진행에 관여하는 것으로 보고되었다. 본 연구에서는 갑상선 유두암의 방사성요오드치료 내성군에서 임상조직학적인 특징과 *BRAF* 돌연변이 및 *TERT* promoter 돌연변이와 같은 유전적인 변화를

확인해보고자 하였으며 방사성요오드치료 반응군과 비교 분석하여 치료 내성군의 고유한 특징을 찾고자 하였다.

강남 세브란스 병원에서 갑상선 유두암으로 표준치료를 받은 환자들 중 방사성요오드 치료의 누적용량이 >600mCi 이면서 재발 또는 원격전이를 보여 치료 내성을 보인 환자 82명 중 조직 절편을 구할 수 있는 26명을 찾았고, 표준 치료 후 5년 동안 재발하거나 전이하지 않은 갑상선 유두암 환자 82명을 대조군으로 선정하였다.

병리조직학적 소견을 검토한 결과, 방사성요오드 치료 내성군은 종양의 내부와 변연부에서 혈관을 갖지 않은 작은 종양세포의 군집(small cluster)이 빈번히 보였으며 그 양도 치료 반응군에 비해 증가되어 있었다. 세포의 키가 커지고 징 모양으로 돌출하는 hobnail features도 치료 내성군에서 많이 관찰되었고 특히 종양의 중심부에서 높은 빈도로 관찰되었다. 특이하게도, 치료 내성군에서 종양 세포의 세로길이가 길어진 (Height/Width ratio of tumor cell (maximum ≥ 3) 세포들이 빈번히 관찰되었고, 치료 내성군 내에서도 핵이 위치가 위, 가운데, 아래쪽의 순서로 증가하며 분포하는 경향을 보였다. 치료 내성군은 유사분열과 종양세포의 괴사소견도 대조군에 비해 높은 빈도로 관찰되었다. 유전자 검사 결과 치료 내성군에서 53.8% (14/26)에서 *TERT* promoter 돌연변이를 확인했고 치료 반응군에서는 오직 1예에서만 확인되었다. 두 군에서 *BRAF* V600E 돌연변이는 모두 80% 이상으로 확인되었고, 전체 108예 중 13예는 *TERT* promoter와 *BRAF* 돌연변이가 모두 확인되었다. 조직학적 특징들은 *TERT* promoter 돌연변이와도 유의미한 연관성을 나타내었다. 갑상선 유두암의 분자유전학적 신호전달체계와 관련된 단백질에 대한 면역조직화학염색 결과, 요오드 섭취와 관련한 sodium-iodide symporter (NIS)와 갑상선

자극 호르몬 수용체 (TSHR)의 발현, 혈관신생과 관련된 혈관내피세포성장인자 (VEGF)와 혈관내피세포성장인자 수용체 (VEGF2)의 발현, 세포분열 및 증식과 관련이 있는 nuclear factor kappa B (NF-κB)의 발현이 모두 치료 내성군에서 현저히 감소했다. NIS와 TSHR의 발현감소는 특히 방사성요오드 치료 내성과 관련이 있는 것으로 생각되며, 이들 단백의 발현 감소 정도와 조직학적 특징은 다양한 양상으로 음의 상관관계를 보였다. 방사성요오드 치료 내성군에서 의미 있게 관찰된 임상병리학적 및 분자유전학적 변수들은 회귀분석 결과, 종양괴사, *TERT* 돌연변이, small clusters의 증가 (≥20%) 와 세포의 키 증가((Height/Width ratio of tumor cell (maximum≥3)를 보이는 경우 방사성요오드 치료 내성과 유의미한 연관성을 보였고 98.8%의 치료 내성의 양성 예측률을 보였다.

본 연구를 통해 갑상선 유두암의 방사성요오드치료 내성과 관련한 유전자변이와 조직학적 특징을 확인했지만, 방사성요오드 치료 내성의 진단기준 또는 나쁜 예후 인자로서의 기준으로 공식화하기는 어려웠다. 하지만, 추가 연구를 통해 갑상선 유두암의 진단 및 예후 예측에 적용될 수 있다면 이번 연구의 의미가 클 것이라 여겨진다.

핵심 되는 말: 갑상선 유두암, 방사성 요오드 치료 내성, *TERT* promoter 돌연변이, hobnail, micropapillary